Nonlinear Dyn (2007) 48:391–408
DOI 10.1007/s11071-006-9093-1

ORIGINAL ARTICLE

Bifurcation and stability analysis of an anaerobic digestion model

Shuiwen Shen · Giuliano C. Premier · Alan Guwy · Richard Dinsdale

Received: 7 November 2005 / Accepted: 14 June 2006 / Published online: 25 August 2006

Abstract This paper presents the dynamic behaviour of the anaerobic digestion process, based on a simplified model. The hydraulic, biological and physicochemical processes such as those which underpin anaerobic digestion have more than one stable stationary solution and they compete with each other. Further, the attractive domains of the stable solutions vary with the key parameters. Thus, some initial transient process moving toward one stable solution could suddenly move towards another solution, at which a so-call catastrophe takes places (e.g. washout). The paper systematically analyses the stationary solutions with their associated stability, which provides insight and guidance for anaerobic digestion reactor design, operation and control.

Keywords Anaerobic digestion · Bifurcation · Nonlinear dynamics

S. Shen
Ricardo UK Ltd., Cambridge, CB4 1YG, UK

G. C. Premier (✉)
School of Technology, University of Glamorgan, CF37 1DL, Pontypridd, UK
e-mail: gcpremier@glam.ac.uk

A. Guwy· R. Dinsdale
School of Applied Science, University of Glamorgan, CF37 1DL, Pontypridd, UK

1 Introduction

Biological treatment of municipal, agricultural and industrial wastes and the production of energy rich biogas is commonly achieved using anaerobic digestion. The process relies on complex and synergistic interactions between several functional groups of bacteria. The bacteria metabolise and stabilise these substrates in the absence of oxygen through a series of chemical physicochemical and biochemical reactions and produce carbon dioxide and usable methane [20]. The use of high-rate anaerobic digestion is often restricted by its reputation as a complex and sensitive process even though there are recognised advantages of net energy production and substantially lower sludge production compared to aerobic treatment. Practical control of anaerobic digestion is essential in avoiding the instability which exists in certain regions of operation which may be visited due to inappropriate operation in seeking high productivity [4, 28], or unavoidable disturbances caused by loading rate variations, toxicity and therefore inhibition from the influent, hydraulic shocks, product inhibition (such as volatile acids, ammonia or hydrogen) or pH inhibition [25].

Anaerobic digestion has been the subject of considerable research effort, not least in the area of modelling, where the need for such abstraction has been recognised by many researchers [3, 8]. The Anaerobic Digestion Model No. 1 presented by Batstone [8], while accepting they had omitted several constituent processes, nonetheless had 32 dynamic state variables.

Perhaps because of this complexity, only a few analyses of the nonlinear dynamics of anaerobic digestion have been reported [31]. It is well known that control of nonlinear systems requires deep insight into their dynamics [27]. This is particularly true when coexisting equilibria compete for stability [22]. A locally linearized model is only able to capture behaviour in the neighbourhood of equilibria and should not be used to represent the system if the distances from equilibria become large [5, 21, 27]. Imbalance, for example, between the rate of production of volatile acids and their consumption can lead to the acidification of the anaerobic digestion process, inhibition of methanogenisis and consequently catastrophic failure. Besides, nonlinear system dynamics are often parameter dependent [21], as is the case in anaerobic digestion. For example, a reactor may become unstable as a result of an increased loading rate. Therefore, analysing the nonlinear dynamics of the anaerobic digestion is important and should provide useful guidance for process design, operation and control.

The raising demands of effluent quality standards and the costs associated with discharge, energy, chemicals, plant utilisation and personnel point to the increasing need to develop high-performance control systems. Widespread adoption, however, requires the adequate solution of several engineering problems. Firstly, the process kinetics w.r.t. the growth rate of bacterial population at the extremes of operation are not well understood or reported nonlinear mechanisms. The situation is worsened by the fact that the associated parameters of kinetic functions are time-varying and history dependant in a manner which is ill defined but often described in terms of acclimatisation or population shift. Secondly and notwithstanding recent improvements in sensor technology, reliable on-line sensors, which are needed for advanced control, are either not available or very costly. Thirdly, disturbances w.r.t. the composition, concentration and toxic/inhibitory content of the influent are random and very difficult to observe [1, 7].

As might be expected, the objectives of control in anaerobic digestion related to the process objectives which may include the stable operation of the process, optimal stabilisation of a waste stream such as activated sludge from waste water treatment, maximising the production of energy gasses such as methane and hydrogen or other products such as organic acids. Several trends can be discerned from the literature with regard to the control of these complex nonlinear systems: (1) adaptive systems attempts to estimate the influent disturbances [26], the parameters [7, 12], the state variables [9, 10] and/or kinetics [11, 14, 15] on-line. With the information estimated, a PID like, or more sophisticated control strategies can be readily applied; (2) robust and optimal control [13, 28], on the other hand, is based only on simplified linear models used to develop a feedback law to treat nonlinearities, parameter variations and load disturbances, while (3) feedback linearization or similar [4, 24, 29] is employed to compensate the known nonlinear kinetics through certain implied information contained in (on-line) measurable parameters such as the off gases; and (4) intelligent control system [17, 18, 30] utilises the experiences gained from the reactor operation. It is worth noting that the robust interval-based estimate and regulation proposed by Alcaraz-Gonzalez [1] requires little information about the system but exhibits certain performance under various uncertainties. However, despite the different control strategies that have been applied in the face of incomplete system knowledge, the task of designing a control law to ensure robustness against load disturbances and parameter variations is in general still difficult and requires continuing research efforts.

This paper aims to systematically analyse the stability and bifurcations of a two-population model of the anaerobic digestion process. The rest of the paper is organised as follows. Two-population models are widely used in the anaerobic digestion process analysis and control [1, 4, 16, 23], and one such model is presented in Section 2. This model is reduced to a two-dimensional model in Section 3 and this is followed by a primary stability and phase space portrait analysis in Section 4. After presenting the basic principle of bifurcation in the anaerobic digestion system, bifurcation analysis in the one-dimensional parameter spaces is conducted in Section 5 while Section 6 presents the results of the analysis in the two-dimensional parameter spaces. The paper concludes in Section 7 and offers suggestions for future studies in reactor design, operation and control.

2 Two-population anaerobic digestion model

The anaerobic digestion process is essentially based on a complex chain of bio- and physico-chemical reactions through which the organic substrates are firstly disintegrated and hydrolysed then transformed into volatile fatty acids (VFAs), and subsequently converted into

methane and carbon dioxide. Deterministic lumped parameter models of the process assist in the understanding of catastrophic failure, and help to improve the operation and control of anaerobic digestion processes. ADM1 [8] successfully captures the necessary dynamics of the system, but this model is far too complex for analysing nonlinear dynamics such as that presented in this paper. Thus, a two-population model, representing two species of bacteria (acidogens and methanogens), developed by Marsili-Libelli and Beni [16], is adopted as a starting point and adapted in this research. This model includes: (1) the association and dissociation of acetic acid and sodium bicarbonate; (2) the gas transfer between liquid and gas phases; and (3) the effects of the CO_2 and bicarbonate on the liquid phase pH. However, the adoption of only one functional group of acidogenic bacteria (namely acetogens), over a more highly speciated set of volatile fatty acid producers as in e.g. ADM1, is a noteworthy simplification. Also, the omission of hydrolysis and disintegration of particulate feed, which together proceed under the action of several extracellular enzymatic, chemical and physical processes are important, particularly as these processes can be rate limiting in anaerobic digestion. The main assumptions made and consequent losses of generality for this model are summarized as follows.

$A1$: The organic substrate influent to the reactor is soluble and readily hydrolysed. The disintegration and hydrolysis of particulate substrate is not considered, which limits the model to easily degradable organic substrates.

$A2$: The pathways of the biological process are represented by only two species of bacteria. Acidogenic bacteria X_a which utilise organic substrate S and break it down to produce volatile fatty acids which are all assumed to be acetic acid V_a, and carbon dioxide C which represents the only inorganic component present in the reactor. Methanogenic bacteria X_m grow on acetic acid and break it down into the products, methane and carbon dioxide. Hydrogen is produced by obligate H_2 producing bacteria and volatile fatty acids (mainly propionic, butyric and acid) are also produced during anaerobic digestion, but these and other products are not included in this model.

$A3$: There is no difference between the concentrations of the substrates, biomass populations and volatile acid, in the reactor and at the effluent, implying a CSTR (continuous stirred tank reactor) configuration with hydraulic and solid retention being equal.

$A4$: The liquid and gas volume remain constant as the influent and effluent flow rates remain constant, as does the dilution rate.

$A5$: The total pressure of the gas equals atmospheric pressure, according to Dalton's Law of Partial Pressures.

The variables in the model are given in Table 1, where S, X_a, V_a, X_m, C and P_c are states, Q_{ch_4}, Q_{co_2} and pH are outputs, S_i and B_{ic} are inputs. The necessary coefficients, parameters, their nominal value and an explanation for these are presented in Appendix A. The simplified system dynamics is governed by the

Table 1 Variables of the anaerobic digestion model

S	[mg/l]	Organic substrate concentration
X_a	[mg/l]	Acidogenic bacteria concentration
V_a	[mg/l]	Acetic acid concentration
X_m	[mg/l]	Methanogenic bacteria concentration
C	[mg/l]	Carbon dioxide concentration (liquid phase)
P_c	[atm]	Carbon dioxide partial pressure (gas phase)
Q_{ch_4}	[l/h]	Methane gas production
Q_{co_2}	[l/h]	Carbon dioxide gas production
H_a	[mg/l]	Undissociated fraction of V_a
$[H^+]$	[mg/l]	Cation ions conentration
pH	[–]	pH level of the reactor
S_i	[mg/l]	Influent organic substrate concentration
B_{ic}	[mg/l]	Cation ions conentration introduced by sodium bicardonate

following differential equations:

$$\frac{dS}{dt} = D(S_i - S) - f_a(S, S_i)X_a Y_a \tag{2.1}$$

$$\frac{dX_a}{dt} = [f_a(S, S_i) - D_a]X_a \tag{2.2}$$

$$\frac{dV_a}{dt} = -DV_a + f_a(S, S_i)X_a y^a_{vf} - f_m(H_a)X_m Y_m \tag{2.3}$$

$$\frac{dX_m}{dt} = [f_m(H_a) - D_m]X_m \tag{2.4}$$

$$\frac{dC}{dt} = -DC + f_a(S, S_i)X_a y^a_{\mathrm{co}_2} + f_m(H_a)X_m y^m_{\mathrm{co}_2} - k_{la}(C - k_h P_c) \tag{2.5}$$

$$\frac{dP_c}{dt} = k_g\big[k_{la}(1 - P_c)(C - k_h P_c) - r_g P_c f_m(H_a)X_m y^m_{\mathrm{ch}_4}\big] \tag{2.6}$$

while the outputs of the system are given by

$$Q_{\mathrm{ch}_4} = k_g r_g f_m(H_a)X_m y^m_{\mathrm{ch}_4} \tag{2.7}$$

$$Q_{\mathrm{co}_2} = k_g k_{la}(C - k_h P_c) \tag{2.8}$$

$$\mathrm{pH} = -\log_{10}([H^+]) \tag{2.9}$$

in which

$$\begin{aligned} Y_a &= y^a_{vf} + y^a_{\mathrm{co}_2} + 1/y^a_s \\ D_a &= \delta D + k_{da} \\ Y_m &= y^m_{\mathrm{ch}_4} + y^m_{co_2} + 1/y^m_s \\ D_m &= \delta D + k_{dm} \\ k_g &= \frac{S_v V}{C_{\mathrm{co}_2} V_g} \\ r_g &= \frac{C_{\mathrm{co}_2}}{C_{\mathrm{ch}_4}} \end{aligned}$$

$$f_a(S, S_i) = \frac{\mu^a_{\max} S}{k_{sa} + S}\frac{k_{sa} + S_i}{S_i} \tag{2.10}$$

$$f_m(H_a) = \frac{\mu^m_{\max} H_a}{H_a + k_{sm} + H_a^2/k_{im}} \tag{2.11}$$

A modified Monod kinetic function f_a is used to represent the growth rate of the acidogenic bacterial population. However, the growth rate f_m for the methanogenic bacterial population is represented by a Haldane kinetic function [2], which is commonly applied to describe kinetic behaviour characterised by inhibition. The growth rate function f_m is one of the most complex parts of the model and depends on concentrations of acetic acid V_a and cation ions ($[H^+]$, which naturally translate logarithmically to pH).

$$H_a = \frac{V_a[\mathrm{H}^+]}{k_a + [\mathrm{H}^+]} \tag{2.12}$$

The hydrogen cation concentration $[H^+]$ is governed by the following implicit ion balance function f_h:

$$[\mathrm{H}^+]^3 + (k_a + B_{ic})[H^+]^2 - [k_a(V_a - B_{ic}) + k_w + k_h k_{\mathrm{co}_2} P_c][\mathrm{H}^+] = k_a\big(k_w + k_h k_{\mathrm{co}_2} P_c\big) \tag{2.13}$$

Given the fact that $B_{ic} \geq 0$, $V_a \geq 0$ and $P_c \geq 0$, there is only one feasible solution, namely $[\mathrm{H}^+] > 0$, according to the above implicit function.

Figure 1 shows the growth rates of X_m w.r.t. acetic acid concentration for $\mathrm{pH} \in [5, 8]$. The growth rate increases almost monotonously at more alkali conditions (i.e. $\mathrm{pH} \geq 6.5$). On the other hand, inhibition and saturation play a part when the environment becomes acidic or beyond the neutral condition. Due to the nonlinear characteristics of the growth rate f_m, the overall dynamics becomes rich and complex. The reason for adding sodium bicarbonate is to keep the environment favourable to the methanogenic bacteria, which affects the overall dynamics, primarily by maintaining a balance between the production and consumption of volatile acids.

The fermentation process can be broken into two steps, and each step has one group of bacteria breaking down the respective influent substrate and so reducing the effluent COD (Chemical Oxygen Demand). Acidogenic bacteria produce not only substrate (V_a) for, but also H^+ ions affecting the growth rate of methanogenic bacteria. Thus, the dynamics associated with methanogenic bacteria cannot be independent of the dynamics associated with the acidogenic bacteria. However, the reverse is not true, provided that product inhibition is neglected as is the case in the simplified model. This gives an opportunity to look at the dynamics for acidogenic bacteria independently (notwithstanding the assumptions made) in the following section.

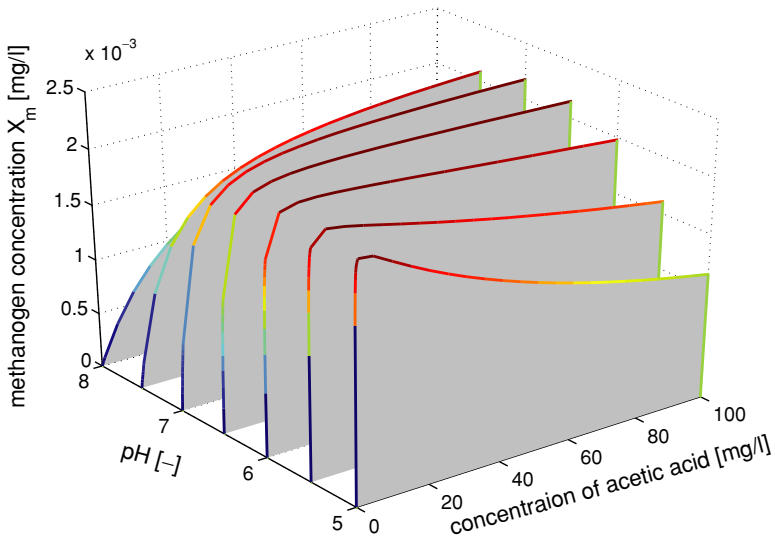

Fig. 1 The growth rate of X_m

3 Two-dimensional anaerobic digestion model

The six-dimensional dynamic presented by Eqs. (2.1)–(2.6) with nonlinear kinetics is very difficult for analysis. Therefore, it is the task of this section to simplify the model by reducing and/or eliminating the two stable and rapid dynamic dimensions.

3.1 The dynamic behaviour of the acidogenic bacterial population

The dynamics associated with acidogenic bacteria, which is governed by Eqs. (2.1) and (2.2), has two fixed-point solutions, i.e.

$S_{a,1}$: $X_{a,1} = 0$ and $S_1 = S_i$.
$S_{a,2}$: $\{S_2 | f_a(S_2, S_i) = D_a\}$ and $X_{a,2} = \frac{D(S_i - S_2)}{D_a Y_a}$.

The stability of the solutions is determined by Jacobian matrix

$$J(X_a, S) = \begin{bmatrix} -(D + \frac{\partial f_a}{\partial S} X_a Y_a) & -f_a Y_a \\ \frac{\partial f_a}{\partial S} X_a & f_a - D_a \end{bmatrix} \tag{3.1}$$

at each fixed-point $(S_k, X_{a,k})$, $k = 1, 2$. Within the domain of $X_a \geq 0$, $S \geq 0$ and $\mu^a_{\max} > D_a$, solution $S_{a,2}$ is stable as $\frac{\partial f_a}{\partial S} > 0$ while $S_{a,1}$ is unstable as a result of $f_a - D_a = \mu^a_{\max} - D_a > 0$. The system is not well defined when $S_i = 0$. It probably undergoes a *transcritical bifurcation* at such a condition, but it is of marginal interest as in practice $S_i > 0$ unless the system is idle. Based on the following facts ($F1$–$F3$), it is reasonable to reduce the dynamics to just a linear functions of infulent concentration S_i, w.r.t. acidogenic bacteria concentration X_a.

$F1$: In the case of easily degradable organic substrates, the dynamics associated with acidogenic bacteria is much faster than those of methanogenic bacteria, as evidenced from their respective growth rates (the growth rate of acidogenic bacteria is about 200 times that of methanogenic bacteria)

$F2$: Although this system has two fixed-point solutions, only $S_{a,2}$ is stable under feasible operating conditions.

$F3$: As shown in Fig. 2(b), the concentration of bacteria X_a is almost linearly dependent on the substrate influent concentration while the concentration of substrate in Fig. 2(a) tends to saturate.

$$X_a = \frac{D}{D_a Y_a} S_i \tag{3.2}$$

Equation (3.2) is employed here to represent the linear relation. The approximate linear relation is also shown in Fig. 2(b) for comparison and can been seen to represent the system well for most of the region shown. Equation (3.2) implies that the effluent concentration is low compared to the substrate concentration at the ingress. This is a reasonable supposition in the case of efficient bacterial action, but deviation should be expected where acidogenic efficiency is degraded, which

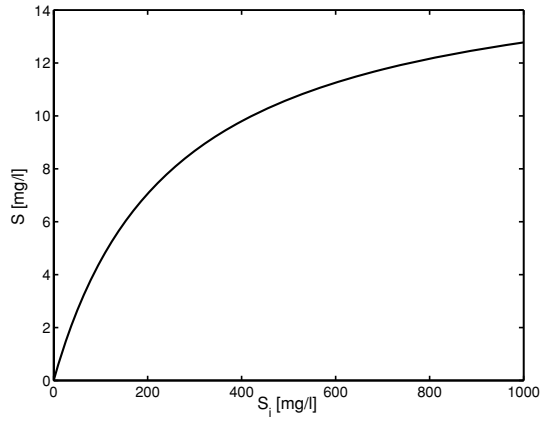

(a) steady-state S

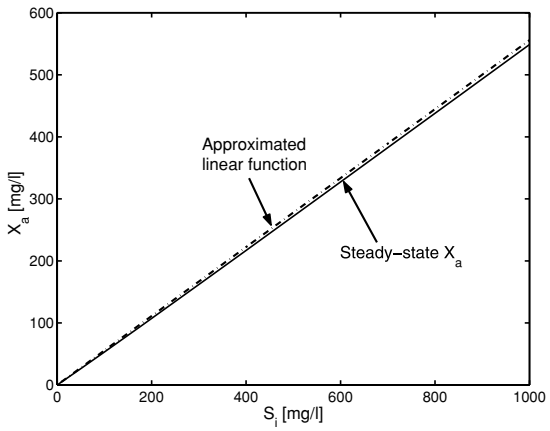

(b) steady-state X_a

Fig. 2 Solution $S2$ against influent concentration S_i

normally occurs as a consequence of stress in the slower methanogenic bacteria.

3.2 The dynamics of gas transfer between the liquid and gas phases

Taking advantage of the simplified dynamics presented in the previous section and applying

$$f_a(S, S_i)X_a = \frac{D}{Y_a}S_i \tag{3.3}$$

to Eq. (2.3) and (2.5), the six-state model is reduced to a four-state model. However, a fourth order system is still some way from easy and illuminating analysis and further reduction is required. Noticing that the dynamics of liquid to gas carbon oxides transfer is far more rapid than the dynamics associated with the methanogenic bacteria, it is possible to reduce the order further. The analysis is simplified by the fact that the effect of the term of the DC at Eq. (2.5) is negligable compared to the term of $k_{la}C$, and gives rise to the following equations:

$$\frac{dC}{dt} = y_{\mathrm{co}_2}DS_i + f_m(H_a)X_m y^m_{\mathrm{co}_2} - k_{la}(C - k_h P_c)$$
$$\frac{dP_c}{dt} = k_g\left[k_{la}(1 - P_c)(C - k_h P_c) - r_g P_c f_m(H_a)X_m y^m_{\mathrm{ch}_4}\right]$$

in which $y_{\mathrm{co}_2} = y^a_{\mathrm{co}_2}/Y_a$. Assuming that S_i and $f_m(H_a)X_m$ are inputs, a fixed-point solution of the system is given by

$$C^* = \frac{y_{\mathrm{co}_2}DS_i + f_m(H_a)X_m y^m_{\mathrm{co}_2} + k_{la}k_h P^*_c}{k_{la}} \tag{3.4}$$

$$P^*_c = \frac{y_{co_2}DS_i + y^m_{co_2}f_m(H_a)X_m}{y_{co_2}DS_i + \left(y^m_{co_2} + r_g y^m_{ch_4}\right)f_m(H_a)X_m} \tag{3.5}$$

Bearing in mind that by neglecting the DC term, a fixed-point for $P_c \in [0, 0.01)$ is lost (see Appendix B for the proof of its existence). However, the lost solution rarely occurs in reality, as such low partial pressure of CO_2 are only likely if anaerobiosis is yet to evolve CO_2. Also, this solution is only stable for very low concentration of substrate influent, which are not typical in anaerobic digestion operations. At steady-state partial pressure *circa* $P^*_c = 0.4$ [atm], and alters little with reactor operation once overall system stability is established, otherwise, $P^*_c = 1$ if instability occurs.

System stability is determined by the following Jacobian matrix:

$$J(C^*, P^*_c) = \begin{bmatrix} -k_{la} & k_{la}k_h + \dfrac{\partial f_m}{\partial P_c}X_m y^m_{\mathrm{co}_2} \\ k_g k_{la}(1 - P^*_c) & -k_g \spadesuit \end{bmatrix} \tag{3.6}$$

in which

$$\spadesuit = k_{la}[(C^* - k_h P^*_c) + k_h(1 - P^*_c)] + r_g X_m y^m_{ch_4}\left[f_m(H_a) + P^*_c\frac{\partial f_m}{\partial P_c}\right]$$

The determinant of the matrix is given by Jacobian matrix

$$\mathbf{Det}(J) = k_g k_{la}\Bigg[y_{co_2} DS_i + \frac{\partial f_m}{\partial P_c} X_m \big(r_g y^m_{ch_4} - y_{co_2}\big) + \big(r_g y^m_{ch_4} + y^m_{co_2}\big) f_m(H_a) X_m\Bigg]$$

Within the operating region of the reactor and with the fact that $\frac{\partial f_m}{\partial P_c} > 0$, the fixed-point solution is stable as $\mathbf{Det}(J) > 0$ and $\mathbf{Tr}(J) < 0$. It is unlikely that a limit cycle exists due to the fact that no *Hopf bifurcation* could take place as $\mathbf{Tr}(J) \neq 0$. Motivated by this intuition, the proof of global stability of the fixed-point solution is given in Appendix B. As a consequence, it is reasonable to reduce two-dimensional dynamics to one dimension, as is described by the following equation:

$$\frac{dP_c}{dt} = k_g\big[(1 - P_c)\big(y_{co_2} DS_i + f_m(H_a) X_m y^m_{co_2}\big) - P_c r_g f_m(H_a) X_m y^m_{ch_4}\big] \tag{3.7}$$

or to a dimensionless nonlinear function as given by Eq. (3.5) by replacing P_c^* with P_c.

3.3 The two-dimensional model dynamics associated with methanogenic bacterial population

According to the above analysis, it is reasonable to reduce the overall dynamics of anaerobic digestion to only two dimensions governed by Eqs. (2.3) and (2.4). Since the dynamics associated with acidogenic bacterial population and the dynamics of the gas–liquid phase transfer are stable and rapid, they are represented by the dimensionless algebraic Eqs. (3.2)–(3.3), and (3.4)–(3.5), respectively. However, after this order reduction, the dominant dynamics of the methanogenic bacteria are the main components left and are also the most complex and interesting elements of the study of the anaerobic digestion dynamics. The insight from these dynamics could provide guidance to design and control of anaerobic digestion reactors. The two-dimensional model is summarised in conjunction with algebraic Eqs. (2.12), (2.13) and (3.5), as follows:

$$\begin{pmatrix} \dot{V}_a \\ \dot{X}_m \end{pmatrix} = \mathbf{F}(V_a, X_m, B_{ic}, S_i, D) = \begin{pmatrix} -DV_a + y_{vf} DS_i - f_m(H_a) X_m Y_m \\ [f_m(H_a) - D_m] X_m \end{pmatrix} \tag{3.8}$$

in which $y_{vf} = y^a_{vf}/Y_a$, V_a, X_m are states, and B_{ic}, S_i, D are parameters. The anaerobic digestion represented by this two-dimensional system has more than one equilibrium in most of the operating regions. The stability of equilibrium heavily depends on the parameters B_{ic}, S_i and D. The stability and bifurcations are analysed in the following sections.

4 Stability and phase space analysis

Fixed-point solutions or equilibria of the anaerobic digestion system are pairs of (V_a, X_m) satisfying $\mathbf{F}(V_a, X_m, B_{ic}, S_i, D) = 0$. Parameters B_{ic}, S_i and D apparently impact on system's fixed-point solutions. In particular, depending on the parameters, the system could have one, two or three fixed-point solutions (and/or equilibria), which are denoted by the following:

$S_{m,1}$: $X_{m,1} = 0$ and $V_{a,1} = y_{vf} S_i$.
$S_{m,k}$: $\{V_{a,k} | f_m(H_a) = D_m\}$ and $X_{m,k} = \frac{D(y_{vf} S_i - V_{a,k})}{D_m Y_m}$, $(k = 2, 3)$.

$S_{m,1}$ is a trivial solution (washout) while $S_{m,2}$ and $S_{m,3}$ are mainly determined by the Haldane kinetic function f_m, but this is not straightforward. The right-hand side of Eq. (3.8), at steady state, implies a map $\zeta : (V_a, S_i, D) \longmapsto X_m$. Considering the fact that $f_m(H_a) = D_m$ at stationary, Eq. (3.5) is the same with a map $\xi : (X_m, S_i, D) \longmapsto P_c$. As aforementioned, the implicit ion balance function f_h has an unique feasible solution for $[H^+]$ and thus defines a map $\varsigma : (V_a, B_{ic}, Pc) \longmapsto [H^+]$. Introducing a map $\pi = \zeta \circ \xi \circ \varsigma$, then according to the function composition $\pi : (V_a, B_{ic}, S_i, D) \longmapsto [H^+]$. Similarly, a map $\varpi : (V_a, [H^+]) \longmapsto H_a$ is defined by Eq. (2.12) while a map $f_m : H_a \longmapsto I_m$ by Eq. (2.11), where I_m is introduced to represent the value of the Haldane inhibition

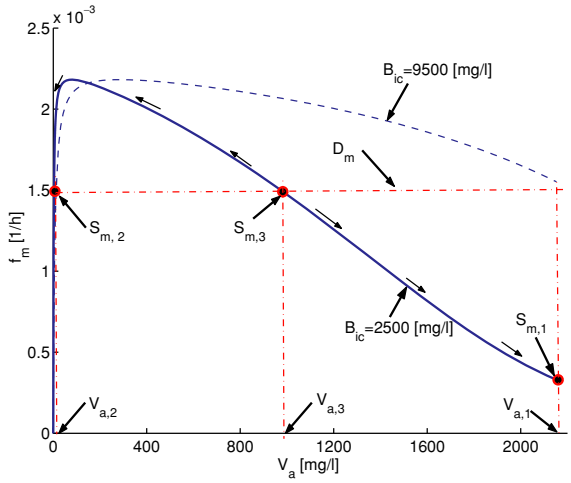

Fig. 3 Growth rate of X_m vs. V_a ($S_i = 12{,}000$ [mg/l])

function. As a result of function composition, kinetic function f_m actually defines a map

$$f_m : (V_a, B_{ic}, S_i, D) \longmapsto I_m \tag{4.1}$$

in steady state, in which V_a is treated as variable, B_{ic}, S_i, D as parameters, while X_m and P_c become only intermediate variables. The fixed-point solutions $S_{m,2}$ and $S_{m,3}$ satisfy

$$f_m(V_a, B_{ic}, S_i, D) = D_m$$

Figure 3 illustrates an example of the function f_m numerically for $S_i = 12{,}000$ [mg/l] and for respective B_{ic} concentrations. The fixed-solutions $S_{m,1}$, $S_{m,2}$ and $S_{m,3}$ are also shown. Typically, the system has three equilibria as those shown in Fig. 3. However, when parameters vary, the system could have only one or two solutions. For instance, f_m bends upward when B_{ic} increase. As a result, $S_{m,3}$ moves to the left (i.e. $\frac{\partial V_{a,3}}{\partial B_{ic}} > 0$) along the line defined by parameter D (actually D_m) in Fig. 3. At a certain level of B_{ic}, solution $S_{m,3}$ touches solution $S_{m,1}$. $S_{m,3}$ then disappears if B_{ic} increase beyond this level. The system has only two fixed-point solutions $S_{m,1}$ and $S_{m,2}$ when $B_{ic} = 9500$ [mg/l] as shown in Fig. 3. Also, $S_{m,2}$ moves left but at a rather slow rate comparing with that of $S_{m,3}$. Similarly, when varying parameter D, the line defined by D_m will change accordingly. For example, this line lifts up when D increases. Consequently, $S_{m,2}$ and $S_{m,3}$ moves toward each other (i.e. $\frac{\partial V_{a,2}}{\partial D} > 0$ and $\frac{\partial V_{a,3}}{\partial D} < 0$). When $S_{m,2}$ and $S_{m,3}$ collapse at a certain level of D, they both disappear and $S_{m,1}$ is the only solution left. However, $S_{m,2}$ and $S_{m,3}$ hardly move when S_i varies, but $S_{m,1}$ moves significantly. $S_{m,1}$ moves to the left when S_i decreases. $S_{m,1}$ touches $S_{m,3}$ at a certain level of S_i. $S_{m,3}$ vanishes when S_i decrease further. At extremely low S_i, $S_{m,1}$ reaches $S_{m,2}$ which is located at the far left of Fig. 3. $S_{m,2}$ also vanishes as a result of continuously decreasing S_i. Thus, it is reasonable to conclude that the number of fixed-point solutions depends on the range of parameters B_{ic}, S_i and D operating. Further, a bifurcation will occur when the number of fixed-point solutions vary, which will be addressed in the following sections.

The stability of each fixed-point solution is once again determined by the Jacobian matrix, which is represented by

$$J(V_a, X_m) = \begin{bmatrix} -D & -f_m Y_m \\ 0 & f_m - D_m \end{bmatrix} \tag{4.2}$$

for fixed-point solution $S_{m,1}$, and by

$$J(V_a, X_m) = \begin{bmatrix} -\left(D + \dfrac{\partial f_m}{\partial V_a} X_m Y_m\right) & -D_m Y_m \\ \dfrac{\partial f_m}{\partial V_a} X_m & 0 \end{bmatrix} \tag{4.3}$$

for fixed-point solutions $S_{m,2}$ and $S_{m,3}$, respectively. The stability of the system requires both

1. $\mathbf{Tr}(J) < 0$;
2. $\mathbf{Det}(J) > 0$.

The stability of $S_{m,1}$ is entirely determined by the sign of $f_m - D_m$ while the stability of $S_{m,2}$ and $S_{m,3}$ by the sign of $\frac{\partial f_m}{\partial V_a}$. In detail,

1. $S_{m,1}$ is stable if $f_m - D_m < 0$, unstable otherwise;
2. $S_{m,2}$ and $S_{m,3}$ are stable if $\frac{\partial f_m}{\partial V_a} > 0$, unstable otherwise.

Figure 3 provides a straightforward means to decide the stability, by investigating the slope of curve defined function f_m w.r.t. V_a around the neighbourhood of $S_{m,2}$ and $S_{m,3}$. Apparently, $S_{m,2}$ is stable while $S_{m,3}$ is unstable. Moreover, $S_{m,3}$ separates the stable solutions $S_{m,1}$ and $S_{m,2}$ as shown in Fig. 3. The system initially locating to the left of the neighbourhood of $S_{m,3}$ will be attracted toward $S_{m,2}$ while to the right, toward $S_{m,1}$.

This observation is further supported by the fact that

$$\mathbf{Det}[J(V_{a,3}, X_{m,3})] < 0$$

which indicates $S_{m,3}$ is actually a saddle point. In most of the reactor operating regions, $S_{m,2}$ is a stable node because of

$$\begin{aligned}\Delta &= \mathbf{Tr}(J)^2 - \mathbf{Det}(J)\\ &= \left(D + \frac{\partial f_m}{\partial V_a} X_m Y_m\right)^2 - 4\frac{\partial f_m}{\partial V_a} D_m X_m Y_m\\ &= \left(D - \frac{\partial f_m}{\partial V_a} X_m Y_m\right)^2\\ &\quad + \frac{\partial f_m}{\partial V_a}[(1-\delta)D - k_{dm}]X_m Y_m\\ &\quad > 0 \text{ if } D > \frac{k_{dm}}{1-\delta} = 8.14e^{-4}\end{aligned}$$

It could still be a stable focus if the dilution rate D were really low (i.e. less damped). The stability of the trivial solution is pretty much parameter dependent. As shown in Fig. 3, $S_{m,1}$ is stable when $B_{ic} = 2500$ [mg/l] as $f_m - D_m < 0$ while unstable when $B_{ic} = 9500$ [mg/l] because $f_m - D_m > 0$. A bifurcation occurs at $f_m - D_m = 0$, namely $\mathbf{Det}(J) = 0$, where the stability of $S_{m,1}$ alters and where $S_{m,3}$ collapses. This bifurcation will be investigated further in the next section.

In summary, $S_{m,2}$ is stable while $S_{m,3}$ is unstable, but the stability of $S_{m,1}$ depends on the operating conditions. Equilibrium $S_{m,2}$ is desirable in anaerobic digestion and corresponds to a high methanogenic population able to convert the energy in the substrates into energy rich methane. However, to operate the reactor at conditions converging to $S_{m,1}$ should be avoided as it corresponds to wash-out of bacteria.

Nevertheless, the Jacobian matrix is only suitable for evaluating the local behaviour of the systems if more than one equilibrium exists, which is the case for anaerobic digestion. Phase space portrait methods are particularly useful to study system dynamics globally, when coexisting equilibria compete for stability.

Figure 4 presents a phase portrait, namely trajectories of the system starting at different initial conditions, with influent concentration $S_i = 12{,}000$ [mg/l] and in a (V_a, X_m) coordinative frame. The useful observations are summarised as follows.

1. Phase portrait diagrams are produced from the four-dimensional model developed in Section 3.2 with four states being V_a, X_m, C and P_c, respectively. Initial starting points are indicated by a '+' while the steady-state solutions are indicated by an 'o'. However, the corresponding steady-state solutions $S_{m,1}$, $S_{m,2}$ and $S_{m,3}$ and their stability are in accordance with the previous analysis, as those shown in Fig. 3 and with subsequent bifurcation analysis such as those shown in Fig. 5, in both quantity and

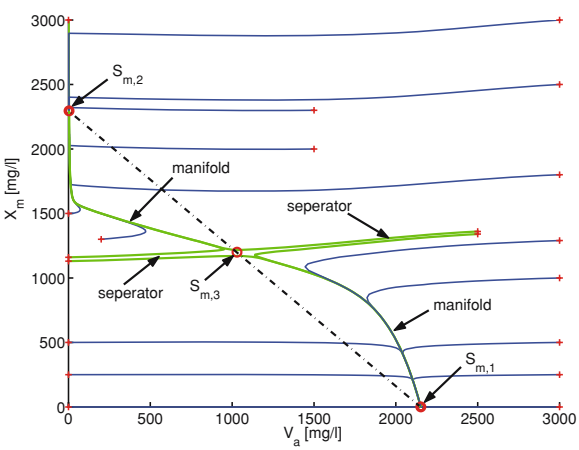

(a) $Bic = 2500$ [mg/1]

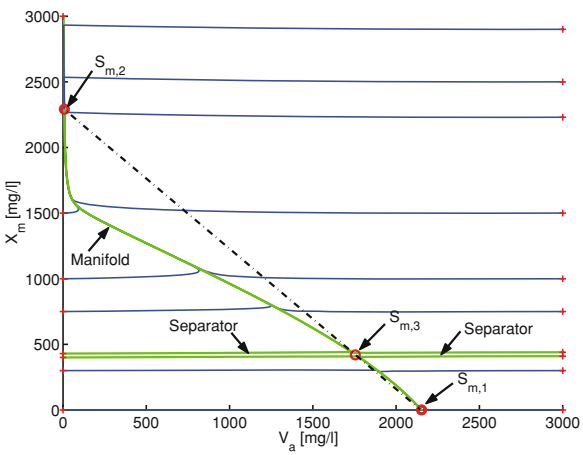

(a) $Bic = 5500$ [mg/1]

Fig. 4 Phase space diagrams for $S_i = 12{,}000$ [mg/l]

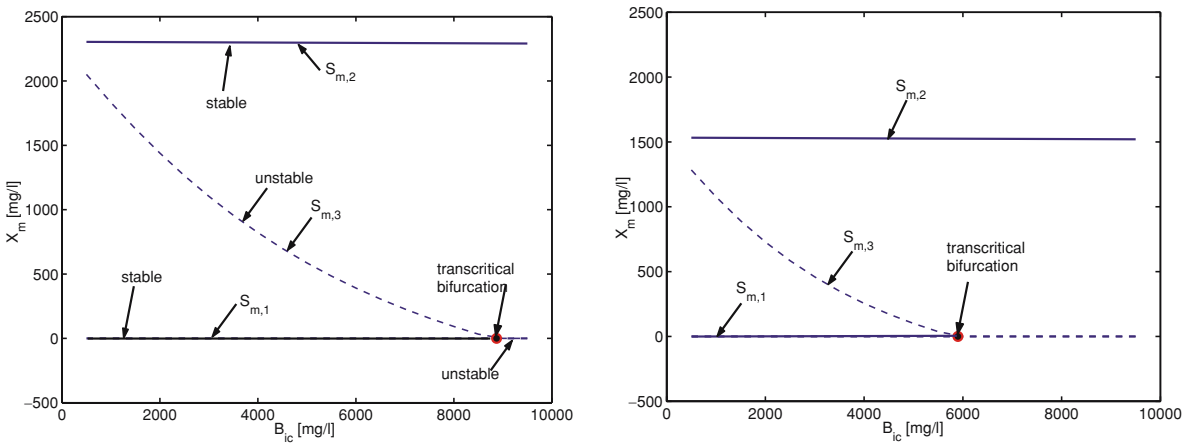

(a) $Si = 12000$ [mg/1] (b) $Si = 8000$ [mg/1]

Fig. 5 Bifurcation map (X_m against B_{ic})

quality. To some extent, the verification of the two-dimensional model is conducted.

2. The insets (or stable manifolds) of the saddle point solution $S_{m,3}$ separate the whole space into the respective attracting domains of stable solution $S_{m,1}$ and $S_{m,2}$. The insets, located between the flows indicated by 'thick green' curves, are not shown on the diagram, but it is possible to produce them numerically by starting the simulation close enough to $S_{m,3}$ and setting the clock to reverse.
3. It is not rigorous to use modes to describe this multi-solution nonlinear system. It is nevertheless possible to observe that V_a varies relatively rapidly while X_m is very slow when initial conditions are at some distance away from the so-called 'manifolds' in diagrams. In addition, Fig. 4(b) provides clear evidence that all the solutions have one eigenvector, obtained by a locally linearised model, which is very nearly parallel to the V_a axis. As a consequence, the attracting domains for the respective stable solutions $S_{m,1}$ and $S_{m,2}$ are dominated by the initial bacterial concentration X_m. Moreover, the eigenvectors of $S_{m,2}$ are nearly orthogonal to each other, and the dynamics near $S_{m,2}$ are almost entirely determined by X_m alone.
4. The overall dynamics essentially display one-dimensional features, as shown in Fig. 4 by the so-called 'manifolds'. The states converge to the manifolds relatively rapidly (taking roughly 6 days depending on the initial conditions), but it takes a very long times (of the order of 120 days) to reach the stable fixed-point solution once on the manifolds. The manifolds are spanned by the unstable manifold of saddle point $S_{m,3}$, and by one of the stable manifolds of node point of $S_{m,1}$ and $S_{m,2}$ when operating near to these stable solutions. The mathematical representation of manifolds and the convergent speed of the system on the manifolds could be obtained analytically or numerically, but will not be addressed in this paper. The rate of convergence could further inform the design, control and operation of the process, provided it is subject to the conditions adopted in this study.
5. Taking the states $V_a = 1700$ [mg/l] and $X_m = 900$ [mg/l] as examples, the comparison of Fig. 4(a) with (b) gives rise to the following valuable conclusion. According to Fig. 4(a), the system is more or less already on the manifold proceeding toward solution $S_{m,1}$ (a wash-out situation). But it is possible to retrieve the situation and make the states become attracted toward $S_{m,2}$, by altering the situation to that represented by Fig. 4(b). This retrieval is based on the fact that the system develops very slowly along the manifold, and that the saddle point solution $S_{m,3}$ is adjustable by parameters such as the alkali buffering represented by B_{ic}.

5 Bifurcation analysis when one of the parameters varies

A bifurcation is where one equilibrium losses or gains stability when parameters change. Typically, the birth

and/or death of an equilibrium is accompanied by a bifurcation. In this section, the dynamic analysis of the anaerobic digestion process is carried out, in particular the impact of the variations of one of the operating parameter B_{ic}, S_i and D, which often lead to bifurcation. Briefly, the Jacobain matrix of the two-dimensional model

$$J(V_a, X_m) = \begin{bmatrix} -\left(D + \dfrac{\partial f_m}{\partial V_a} X_m Y_m\right) & -f_m Y_m \\ \dfrac{\partial f_m}{\partial V_a} X_m & f_m - D_m \end{bmatrix} \tag{5.1}$$

determines the stability of the system locally, namely around equilibria. The Jacobain matrix does nothing more than represent a linear space tangent to the nonlinear space defined by $\mathbf{F}(V_a, X_m, B_{ic}, S_i, D)$ at the given equilibria. Since equilibria $S_{m,k}$ $(k = 1, 2, 3)$ themselves are determined by these operating parameters as shown at the beginning of Section 4, it is therefore reasonable to conclude that the Jacobain matrix can be entirely parameterised by B_{ic}, S_i and D at the given equilibria, i.e.

$$J(V_{a,k}, X_{m,k}) = J_k(B_{ic}, S_i, D),\ k = 1, 2, 3$$

in which J_k represent the Jacobian Matrix at the k-th equilibrium. As mentioned previously, the stability of one equilibrium requires both $\mathbf{Tr}(J) < 0$ and $\mathbf{Det}(J) > 0$. The equilibrium loses stability if one of the conditions is not satisfied. Thus, the bifurcation occurs if

1. $\mathbf{Tr}(J) = 0$, or
2. $\mathbf{Det}(J) = 0$.

as a result of respective or simultaneous variation of the parameters B_{ic}, S_i and D. *Co-dimensional One* bifurcation takes place when either of the conditions are met while *Co-dimensional Two* bifurcation occurs when both the conditions are satisfied. Condition 2 leads to *transcritical* and/or *saddle-node bifurcation*. On the other hand, condition 1 could give birth to a *Hopf bifurcation*, which in turn introduces limit cycles. *Hopf bifurcation* requires both $\mathbf{Tr}(J) = 0$ and $\mathbf{Det}(J) > 0$, but it is not possible since the former requires for $\frac{\partial f_m}{\partial V_a} < 0$ and the latter $\frac{\partial f_m}{\partial V_a} > 0$, which are contradictory. Thus, limit cycles are not likely to happen, and attentions of this study are in the *transcritical* and *saddle-node bifurcation* analysis. The section is organized such that the bifurcation w.r.t. variations of the parameters sodium bicardonate B_{ic}, influent substrate concentration S_i and dilution rate D, respectively, are considered.

5.1 Bifurcation analysis w.r.t. the variation of B_{ic}

Figure 5 shows bifurcation diagrams, in which methanogenic bacterial concentration X_m is taken as one axis and sodium bicardonate B_{ic} as the other (i.e. different B_{ic} relates to different pHs through the bicarbonate CO_2 and pH system), for different levels of S_i. According to the diagrams, a *transcritical bifurcation* takes place at a critical level of sodium bicarbonate B_{ic}^*, which is $B_{ic}^* = 8700$ [mg/l] for $S_i = 12{,}000$ [mg/l] while $B_{ic}^* = 5800$ [mg/l] for $S_i = 8000$ [mg/l]. Analytically, the bifurcation points can be identified by the following equation:

$$\{B_{ic}^* | \mathbf{Det}[J_k(B_{ic}^*, S_i, D)] = 0, \quad k = 1, 2, 3\} \tag{5.2}$$

For both diagrams, the system has three equilibria when $B_{ic} < B_{ic}^*$ but only has two when $B_{ic} > B_{ic}^*$. The birth and/or death of solution $S_{m,3}$ takes place when $B_{ic} = B_{ic}^*$, which is also where solution $S_{m,1}$ gain and loses stability depending on which direction the B_{ic} is varied. Moreover, $S_{m,2}$ remain almost the same despite the variation of B_{ic}, but $S_{m,3}$ changes its position in the diagram dramatically. Thus, this means the adding of sodium bicarbonate does not affect the system at steady state, but does affect its dynamics.

Furthermore, the coexisting equilibria $S_{m,1}$ and $S_{m,2}$ compete for stability when $B_{ic} < B_{ic}^*$, which are shown both in Figs. 4 and 5. Depending on the initial and operating conditions, the anaerobic digestion process can eventually settle down to one of the possible solutions. As mentioned in the previous section, but given in Fig. 5 again, the unstable solution $S_{m,3}$ acts as a separator. An initial bacterial concentration above the curve defined by $S_{m,3}$ will be attracted by solution $S_{m,2}$ while the solution $S_{m,1}$ attracts the initial condition below the curve. Thus, solution $S_{m,3}$ determined the attractive domain for $S_{m,1}$ and $S_{m,2}$. Since $S_{m,2}$ is the favourable solution, relating to methane production, it the interesting to enlarge its attracting domain or even make $S_{m,2}$ the only stable equilibrium, which is clearly achievable by appropriately increasing the level of B_{ic}.

5.2 Bifurcation analysis w.r.t. the variation of S_i

It has been shown in Fig. 5 that not only does parameter B_{ic} affect the number of fixed-point solutions and their stability but so does S_i, although this is true only where the influent substrate is readily degradable and hydrolysis and disintegration are dynamically negligible, as the modelling in this study suggests. Figure 6 explores this effect further.

Similar to previous analysis, bifurcation points w.r.t. parameter S_i are S_i^* satisfying

$$\{S_i^* | \mathbf{Det}[J_k(B_{ic}, S_i^*, D)] = 0, \quad k = 1, 2, 3\} \tag{5.3}$$

There are two *transcritical bifurcations* in Fig. 6, one occurring at $S_i^* = 7.5$ [mg/l] while the other at $S_i^* = 3500$ [mg/l]. At each bifurcation, the trivial solution $S_{m,1}$ exchanges its stability with the new fixed-point solutions at their birth. Solution $S_{m,1}$ relinquishes its stability to $S_{m,2}$ at *bifurcation* 1, which is enlarged in the top-left inset of Fig. 6 for clarity. Conversely, solution $S_{m,1}$ regains stability and passes instability to solution $S_{m,3}$ at *bifurcation* 2. Solution $S_{m,3}$ then separates stable solutions $S_{m,1}$ and $S_{m,2}$.

At influent substrate concentrations S_i lower than 7.5 [mg/l], it is not possible to produce any methane since $S_{m,1}$ is the only equilibrium. In such cases, the methanogenic bacterial washout and death rate exceeds their growth rate leading to extinction. Within the region $7.5 < S_i < 3500$ [mg/l], $S_{m,2}$ becomes the only stable solution, suggesting suitable operating conditions for an anaerobic digestion reactor. Accordingly, increasing the substrate concentration S_i leads to a higher methane production. However, if substrate concentration is too high, for instance $S_i > 3500$ [mg/l], a trade-off arises. On the one hand, methane production benefits from high substrate concentration, but on the other hand, the methanogenic bacterial population has to be kept high (by retaining biomass in some way) in order to prevent the system from converging to the trivial (or reactor failure) solution $S_{m,1}$, perhaps due to some disturbances. Thus, unlike the parameter B_{ic}, S_i has to be carefully operated to reach a suitable balance between system robustness and methane productivity.

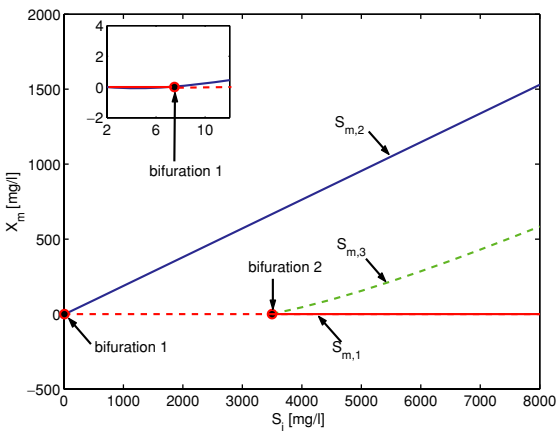

Fig. 6 Bifurcation diagram (X_m vs. S_i, $B_{ic} = 2500$ [mg/l])

5.3 Bifurcation analysis w.r.t. the variation of D

Dilution rate D is an important reactor operating parameter, and an illustration of its effect on system dynamics is given by Fig. 7. There are also two bifurcations in this diagram, a *transcritical bifurcation* occurring at $D^* = 0.04\,\mathrm{h}^{-1}$ and a *saddle-node bifurcation* $D^* = 0.083\,\mathrm{h}^{-1}$. Analytically, the bifurcation point D^* satisfies

$$\{D^* | \mathbf{Det}[J_k(B_{ic}, S_i, D^*)] = 0, \quad k = 1, 2, 3\} \tag{5.4}$$

Within the region of $0.04 < D < 0.083\,\mathrm{h}^{-1}$, once again it is indicated that solution $S_{m,3}$ separates the coexisting stable solution $S_{m,1}$ and $S_{m,2}$. In order to make sure the system operates at solution $S_{m,2}$, initial states must be kept at some distance from $S_{m,3}$, otherwise a small disturbance might turn the system toward $S_{m,1}$, which is certainly a catastrophic condition for anaerobic digestion. Should the system work at

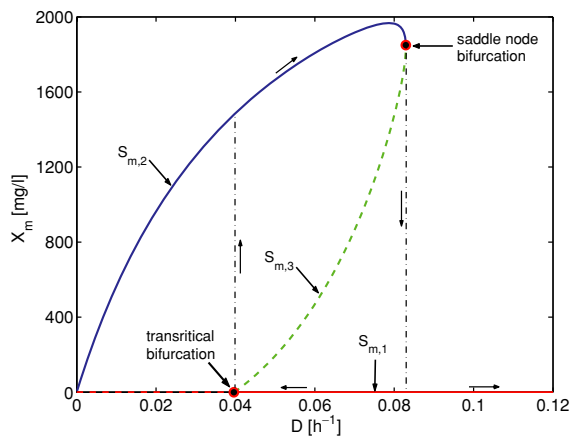

Fig. 7 Bifurcation diagram ($B_{ic} = 5500$ [mg/l] and $S_i = 8000$ [mg/l])

$D < 0.04\,\mathrm{h}^{-1}$, it will not suffer this problem, but suffer from low methanogenic activity and methane production. The most important feature of the dynamics is a catastrophe at the *saddle-node bifurcation*. The reactor would experience a sudden death (washout) if the dilution rate were sufficiently high. At this point, the transition is relatively rapid and it would take a considerable efforts to recover the reactor. Figure 3 also demonstrates this phenomenon. The *saddle-node bifurcation* occurs when $D_m = \mu^m_{\max} = 2.27e^{-3}$, which is the same with $D = 0.083\,\mathrm{h}^{-1}$. There is no other solution than the trivial solution $S_{m,1}$ once $D_m > \mu^m_{\max}$. Also, a small disturbance could lead to this catastrophe when the dilution rate is too close to *saddle-node bifurcation* level $D^* = 0.083\,\mathrm{h}^{-1}$. Thus, it is very important to keep the system away from the critical dilution rate, whether the aim is to control or simply operate the reactor.

In summary, increasing the level of B_{ic} improves the robustness of anaerobic digestion process by either making the favourable solution $S_{m,2}$ the only stable solution or enlarging its attractive domain. Appropriately increasing the influent substrate concentrations S_i and dilution rate D lead to a high methane productivity, but deteriorate the robustness of the system. In particular, increasing the dilution rate D has a risk of running the system at washout condition. Thus, parameters S_i and D must be carefully selected during operation.

6 Bifurcation analysis when two parameters vary simultaneously

Attention so far has been focused on discussing bifurcations when one of the operating parameters (B_{ic}, S_i and D) varies. However, these parameters are likely to vary simultaneously in practice and it is thus more interesting to investigate what the impact of this would be on the system dynamics.

For one or more parameter varying of anaerobic digestion process, a bifurcation takes place when

$$\mathbf{Det}[J_k(B_{ic}, S_i, D)] = 0, \quad k = 1, 2, 3 \tag{6.1}$$

This implicit function actually defines one or more surfaces, on which a bifurcation occurs, in a three-dimensional (B_{ic}, S_i, D) parameter space. These surfaces separate the entire parameter space into several regions. The topological structure of the equilibria, namely the number of equilibria and their associated stability, remains the same in each region. However, it is difficult to display a bifurcation diagram with the variations of all parameters since it essentially requires a four-dimensional coordinate system. Nevertheless, bifurcation surfaces reduce to bifurcation curves in two-dimensional sub-parameter spaces (B_{ic}, S_i), (S_i, D) and (B_{ic}, D), and to bifurcation points in one-dimensional sub-parameter spaces spanned by individual parameter B_{ic},S_i and D. Bifurcations in the one-dimensional sub-parameter spaces have been studied in the previous section. It is the task of this section to look at the bifurcation curves in two-dimensional sub-parameter spaces, in particular the spaces spanned by B_{ic} and S_i, and by S_i and D.

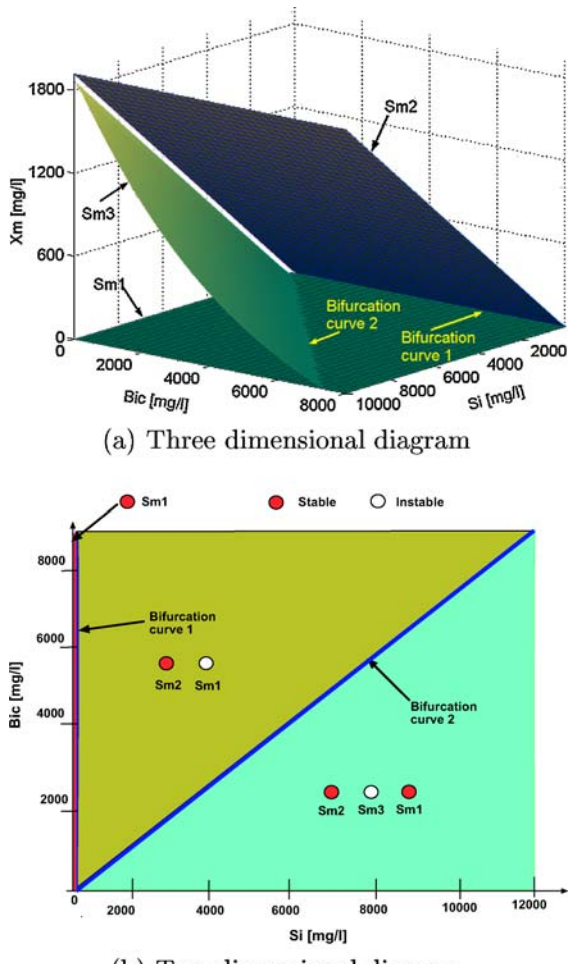

Fig. 8 Bifurcation diagram w.r.t. parameters B_{ic} and S_i

A three-dimensional diagram is given by Fig. 8(a), indicating not only that three fixed-point solutions move with the parameter S_i and B_{ic} and changes their stability accordingly, but so do the bifurcation points. Figures 5 and 6 are effectively orthogonal cross sections of this diagram at given S_i and B_{ic} levels. The so-called *bifurcation curve* 1 is made up of *transcrtical bifurcation* 1, where solution $S_{m,1}$ and $S_{m,2}$ joint (and occurs at very low substrate concentration and hardly moves with B_{ic}). Similarly, *bifurcation curve* 2 collects the possible locations of *transcrtical bifurcation* 2, when varying with both S_i and B_{ic}.

The bifurcation curves divide the spaces spanned by parameter S_i and B_{ic} into different regions, and system dynamics change dramatically once these regional boundaries are crossed. As shown in Fig. 8(b), the system has three fixed-point solutions in the region below *bifurcation curve* 2, in which $S_{m,1}$ and $S_{m,2}$ compete for stability while $S_{m,3}$ is an unstable saddle; two solutions $S_{m,1}$ (unstable) and $S_{m,2}$ (stable) in the region between *bifurcation curves* 1 and 2; only one stable solution $S_{m,1}$ in a very narrow region to the left-hand side of *bifurcation curve* 1. Two bifurcation curves join when there is no substrate at the influent, i.e. $S_i = 0$. For anaerobic digestion reactors, it is certainly necessary to avoid working in the region in which $S_{m,1}$ becomes the only stable solution, which is the case when S_i is extremely low. By contrast, it is preferable to operate the reactor in the region where $S_{m,2}$ is the only stable solution. This is the region between the bifurcation curves. Nevertheless, operating the reactor in the region below *bifurcation curve* 2 should not necessarily be avoided, but care must be taken as the trivial solution is competing to be a stable solution. Figure 8 tells us that solution $S1$ will attract if the initial bacteria population concentration is located somewhere between surfaces defined by solution $S_{m,3}$ and $S_{m,1}$. The following conclusions might be drawn from observation of Fig. 8.

1. The reactor is more stable when running on fairly low substrate concentration conditions, but its performance is limited and characterised by low methane production.
2. The sodium bicarbonate helps in stabilising the reactor when substrate concentration is high.
3. When the reactor runs steadily, sodium bicarbonate can be lowered to reduce the running costs while substrate can be increased to improve throughput and methane productivity. When bicarbonate is too low and substrate concentration is too high, this narrows the attractive domain of the preferable solution $S_{m,2}$, and should be avoided.

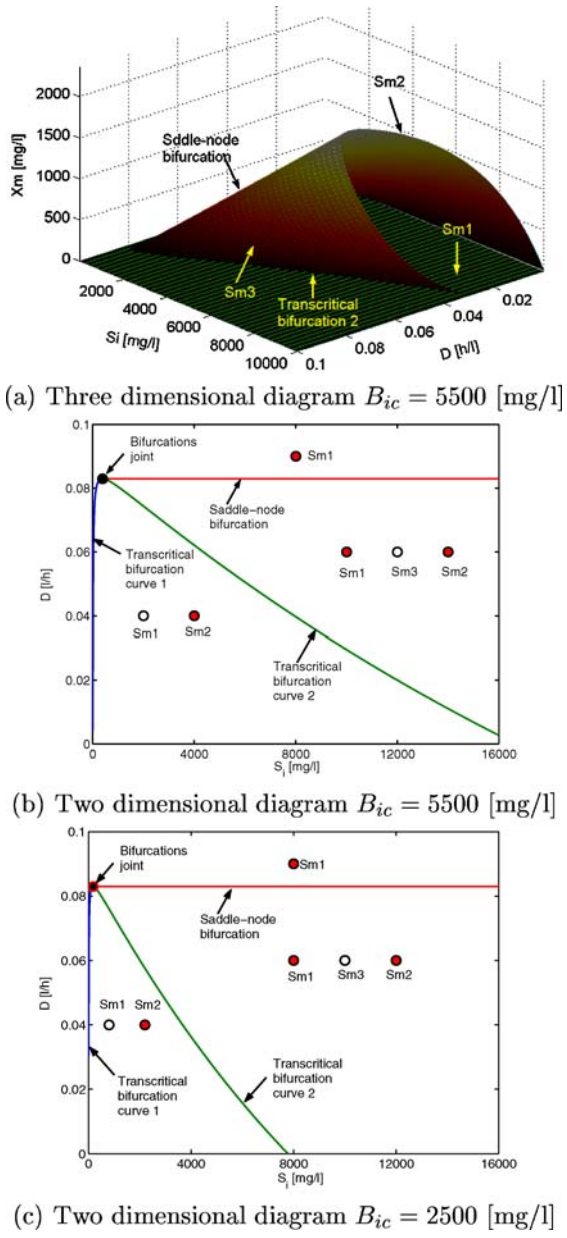

Fig. 9 Bifurcation diagram w.r.t. parameters B_{ic} and S_i

Figure 9(a)–(c) addresses the impact of dilution rate D and substrate concentration S_i. Three bifurcation curves, namely, *saddle-node bifurcation curve*, *transcritical bifurcation curve* 1 and *transcritical bifurcation curve* 2, are clearly shown. Once more,

bifurcation diagrams given by Figs. 6 and 7 are only special cases, at which the bifurcation curves reduce to individual isolated points. Notice that *transcritical bifurcation curve* 1 and *transcritical bifurcation curve* 2 are identical to the respective *bifurcation curve* 1 and *bifurcation curve* 2 presented in Fig. 8, despite the fact that they are presented in different parameter spaces. However, a *saddle-node bifurcation curve* or a *saddle-node bifurcation point* does not appear in Fig. 8, and this is not surprising as the dilution rate D is fixed to a nominal value of $0.042\,\mathrm{h}^{-1}$. Bifurcation curves separate the parameter space into several subspaces. The number of fixed-point solutions and their associated stability remain the same in each subspace, but change dramatically between different subspaces, as is shown at Fig. 9(b) and (c). Higher order codimension bifurcations arise at very low substrate concentrations and high dilution rates, which is the point where bifurcation curves join together. Higher order codimension bifurcation might give birth to a new branch of bifurcation, but will not be addressed in this paper. The observations are summarised as follows:

1 The high dilution rate is of benefit to methane productivity, but may cause the reactor to die if the dilution rate become too high. The reason for this is that the reactor is working in the region that $S_{m,1}$ and $S_{m,2}$ compete for stability and the attractive domain of $S_{m,2}$ becomes rather narrow.
2 Operating the reactor at or near the *saddle-node bifurcation curve* should be avoided as this may result in a small disturbance causing catastrophic failure. However, operating at dilution rates which are too low would not necessarily be preferable, primarily because of low throughput and methane productivity.
3 By comparing Fig. 9(b) and (c), it may be concluded that higher levels of sodium bicarbonate allow the reactor to operate over a wide range of dilution rates and substrate concentrations, but at a financial cost for the alkali addition.
4 To make $S_{m,2}$ the only stable solution often requires the reactor to work on rather low substrate concentrations and low dilution rates, which is contradictory to high-rate reactor requirements for high throughput and high methane production. It is therefore difficult to ensure robustness and productivity simultaneously. If this compromise is considered unsatisfactory, an appropriate control strategy is essential to operate in regions of reduced stability margins.

7 Conclusion

Based on the two-dimensional model developed from the two-population model, it is confirmed that the dynamics of the anaerobic digestion system depends heavily on the Haldane-type kinetic function describing the growth rate of methanogenic bacterial population, and on the key parameters sodium bicarbonate B_{ic}, influent substrate concentration S_i and dilution rate D. Naturally, biomass concentrations X_a and X_m and products which lead to inhibition would also affect dynamics, but have not been investigated here. In the region of the parameters in which the system is operating, there could be one, two or three equilibria. The stability of the equilibria and the bifurcations of the system have been analysed w.r.t. variation of one parameter and then simultaneously variation of two parameters. The useful conclusions from this study are summarised as follows:

First of all, adding sodium bicarbonate B_{ic} to the reactor makes the robustness of the anaerobic digestion process better, by either making the favourable solution $S_{m,2}$ the only stable solution or enlarging its attractive domain. However, increasing the influent substrate concentrations S_i and dilution rate D to maximise methane production will deteriorate the system's robustness. The system displays an inherent trade-off between the robustness and productivity.

Secondly, operating the reactor at or near to the *saddle-node bifurcation curve* should be avoided as this may result in a small disturbance causing catastrophic failure.

Thirdly, higher levels of sodium bicarbonate buffering allow the reactor to operate on a wide range of dilution rates and substrate concentrations, which in turn improve the methane productivity.

Finally, based on the fact that the growth rate of methanogenic bacteria is confirmed to be slow, it is possible to retrieve the system from failure caused by inappropriate operation by altering B_{ic}, S_i and D, respectively or simultaneously.

The last two conclusions are interesting and important as they indicate that the way to design a control strategy for the anaerobic digestion is to consider the

trade-off between robustness and productivity. This can be aided by the clarity provided by the methods of abstractions presented in this study. As the margins to the boundaries of stability can be assessed by this methodology, so the stability margin can be selected and the trade-off quantified albeit in the context of a simplified model of anaerobic digestion.

Appendix A: Parameters and their nominal values

The nominal values of the parameters used in this paper are given in Table 2.

Appendix B: Solution analysis for liquid and gas transfer

In order to yield state-state solution, left-hand side of Eqs. (2.5) and (2.6) are set to zero. by applying Eq. (3.3), it yields,

$$C = \frac{y_{co_2} DS_i + y^m_{co_2} f_m(H_a) X_m + k_{la} k_h P_c}{D + k_{la}}$$

Instituting the above equation into Eq. (2.6) (being aware that the left-hand side is zero), and rearranging it, yields the follows

$$(1 - P_c)\left[\frac{k_{la}}{D + k_{la}}(y_{co_2} DS_i + k_{la} k_h P_c) - k_{la} k_h P_c\right] = f_m(H_a) X_m \left[r_g y^m_{ch_4} P_c - \frac{k_{la} y_{co_2}}{D + k_{la}}(1 - P_c)\right]$$

It is clear that, if the above equation is converted to a function of X_m w.r.t. partial pressure P_c

$$r_g y^m_{ch_4} P_c - \frac{k_{la} y_{co_2}}{D + k_{la}}(1 - P_c) = 0$$

i.e.

$$\hat{P}_c = \frac{1}{1 + r_g\left(1 + \frac{D}{k_{la}}\right)\frac{y^m_{ch_4}}{y_{co_2}}}$$

is a singular point. For the nominal parameters, $\hat{P}_c = 0.01$. bearing in mind that $P_c \in (0, 1)$ in practice, it

Table 2 Parameters used by [16]

Parameter	Value	Unit	Description
$\mu^a_{\max}$	0.5033	[h^{-1}]	Maximum growth rate of acidogenic bacteria
k_{sa}	238.1	[mg/l]	Acidogenic bacteria half-velocity
k_{da}	3.1e^{-2}	[h^{-1}]	Acidogenic bacteria decay rate
$\mu^m_{\max}$	2.27e^{-3}	[h^{-1}]	Maximum growth rate of methanogenic bacteria
k_{sm}	1.45e^{-2}	[mg/l]	Methanogenic bacteria half-velocity
k_{im}	35.47	[mg/l]	Methanogenic bacteria inhibition concentration
k_{dm}	8e^{-4}	[h^{-1}]	Methanogenic bacteria decay rate
y^a_s	0.688	–	Yield coefficient (substrate to acidogenic bacteria)
y^a_{vf}	0.6427	–	Yield coefficient (substrate to acetic acid)
$y^a_{co_2}$	0.5	–	Yield coefficient (substrate to CO_2)
y^m_s	3.27	–	Yield coefficient (acetic acid to methanogenic bacteria)
$y^m_{ch_4}$	20.732	–	Yield coefficient (acetic acid to CH_4)
$y^m_{co_2}$	5.174	–	Yield coefficient (acetic acid to CO_2)
k_w	1e^{-14}	–	Water dissociation constant
k_{co_2}	4.5e^{-7}	–	Carbonic acid dissociation constant
k_h	1.08e^3	–	Henry's law constant
k_a	1.85e^{-5}	–	Weak acid dissociation constant
k_{la}	6.832	–	CO_2 mass transfer rate coefficient
S_v	22.4	–	Avogadro's constant
C_{co_2}	4.4e^4	–	mole to [mg/l] conv const for CO_2
C_{ch_4}	1.6e^4	–	mole to [mg/l] conv const for Ch_4
δ	0.01667	–	Liquid/solid dilution rate ratio
D	0.042	[h^{-1}]	Dilution rate
V	30	[l]	Liquid phase volume
V_g	5	[l]	Gas phase volume
P_t	1	[atm]	Total pressure in the gas phase

therefore has one steady-state solution in the region of (0 0.01) and another in the region of (0.01 1).

Neglecting the term of DC causes the solution in the region of (0.01 1) to disappear, and the other solution becomes globally stable. In order to prove this, the following Lyapunov (semi-positive) function is chosen:

$$f(C, P_c) = a(C - C^*)^2 + b(P_c - P_c^*)^2$$

in which coefficients $a > 0$ and $b > 0$ are underdetermined, and C^* and P_c^* are given by Eqs. (3.4) and (3.5). The proof of global stability is to ensure that $\dot{f} = 0$ at (C^*, P_c^*) and < 0 elsewhere

$$\begin{aligned}\dot{f} &= 2a(C - C^*)\dot{C} + 2b(P_c - P_c^*)\dot{P}_c \\ &= 2a(C - C^*)k_{la}[(C^* - k_h P_c^*) - (C - k_h P_c)] \\ &\quad +2b(P_c - P_c^*)k_g k_{la}\Big[(1 - P_c)(C - k_h P_c) \\ &\quad -\frac{P_c}{P_c^*}(1 - P_c^*)(C^* - k_h P_c^*)\Big]\end{aligned}$$

The common positive term $2k_{la}$ makes no difference w.r.t. proof of the stability, and is moved to the left-hand side of equation

$$\begin{aligned}\frac{\dot{f}}{2k_{la}} &= a(C - C^*)[(C^* - C) + k_h(P_c - P_c^*)] \\ &\quad +bk_g(P_c - P_c^*)\{(1 - P_c)(C - C^*) \\ &\quad +[\Delta + k_h(1 - P_c)](P_c^* - P_c)\} \\ &= -(a\delta C^2 + b^*\delta P^2 - c^*\delta C\delta P)\end{aligned}$$

in which

$$\begin{aligned}\Delta &= \frac{C^* - k_h P_c^*}{P_c^*} \geq 0 \\ \delta C &= (C - C^*) \\ \delta P &= (P_c - P_c^*) \\ b^* &= bk_g\,[\Delta + k_h(1 - P_c)] \geq 0 \\ c^* &= ak_h + bk_g(1 - P_c) \geq 0\end{aligned}$$

If $2\sqrt{ab^*} > c^*$, it is then possible to have new coefficients a_1, a_2, b_1 and b_2 such that $2\sqrt{a_1 b_1} = c^*$, $a_2 = a - a_1 > 0$ and $b_2 = b^* - b_1 > 0$, and to express the right-hand side of the above equation as

$$-[(a_1\delta C - b_1\delta P)^2 + a_2\delta P^2\delta C^2 + b_2\delta P^2] \leq 0$$

The only way to satisfy that the Lyapunov function is equal to zero is at the equilibrium of the system, and therefore the equilibrium is globally stable. There are infinite designs of a and b such that Lyapunov stability statifies, and an example is given as follows:

$$\begin{aligned}a &> 0 \\ b &> \frac{ak_h^2}{4k_g\Delta}\end{aligned}$$

The following shows how the design ensures $2\sqrt{ab^*} > c^*$.

$$\begin{aligned}b &> \frac{k_h^2 a}{4k_g\Delta} \\ &\Leftrightarrow 4abk_g\Delta > a^2k_h^2 \\ &\Leftrightarrow 4abk_g\Delta > [ak_h - bk_g(1 - P_c)]^2 \\ &\Leftrightarrow 4abk_g\Delta + 4ak_h bk_g(1 - P_c) \\ &> [ak_h + bk_g(1 - P_c)]^2 \\ &\Leftrightarrow 2\sqrt{abk_g[\Delta + k_h(1 - P_c)]} > ak_h + bk_g(1 - P_c) \\ &\Leftrightarrow 2\sqrt{ab^*} > c^*\end{aligned}$$

Bearing in mind that the above proof requires $\Delta > 0$, it is easy to show the global stability when $\Delta = 0$, and thus neglected.

References

1. Alcaraz-Gonzales, V., Harmand, J., Rapaport A., Steyer, J.P.: Robust interval-based SISO regulation under maximum uncertainty conditions in an anaerobic digester. In: Proceedings of the 2001 IEEE International Symposium on Intelligent Control. Mexico City, Mexico (2001)
2. Andrews, J.F.: Modeling and simulation of waste-water treatment processes. Water Sewage Works **March**, 62–65 (1975)
3. Andrews, J.F.: Control strategies for the anaerobic digestion process. Water Sci. Technol. **28**, 141–150 (1993)
4. Antonelli, R., Harmand, J., Steyer, J.P., Astolfi, A.: Set-point regulation of an anaerobic digestion process with bounded output feedback. IEEE Trans. Control Syst. Technol. **11**(4), 495–504 (2003)

5. Arrowsmith, D.K., Place, C.M.: An Introduction to Dynamical Systems. Cambridge University Press, Cambridge, UK (1991)
6. Azeiteiro, C., Capela, I.F., Durate, A.C.: Dynamic model simulations as a tool for evaluating the stability of an anaerobic process. Water SA **27**(1), 109–114 (2001)
7. Bastin, G., Dochain, D.: On-line Estimation and adaptive control of Bioreactors. Elsevier, Amsterdam, The Netherlands (1990)
8. Batstone, D.J., Keller, J. et al.: Anaerobic Digestion Model No. 1 (ADM1), IWA Task Group for Mathematical Modelling of Anaerobic Digestion Processes. IWA Publishing, London (2002)
9. Boskovic, J.D.: Observer-based adaptive control of a class of bioreactor processes. In: Proceedings of the 34th Conference on Decision and Control, pp. 1171–1176. New Orleans, LA (1995)
10. Chen, L., Hontoir, Y., Huang, D., Zhang, J., Morris, A.J.: Combining first principles with black-box techniques for reaction systems. Control Eng. Pract. **12**, 819–826 (2004)
11. Farza, M., Busawon, K., Hammouri, H.: Simple nonlinear observers for on-line estimation of kinetic rates in bioreactors. Automatica **34**, 301–318 (1997)
12. Hilgert, N., Harmand, J., Steyer, J.P., Vila, J.P.: Nonparameteric identification and adaptive control of an anaerobic fluidized bed digester. Control Eng. Pract. **8**, 367–376 (2000)
13. Impe, J.F., Bastin, G.: Optimal adaptive control of fed-batch fermentation process. Control Eng. Pract. **3**, 939–954 (1995)
14. Guay, M., Dochain, D., Perrier, M.: Adaptive extremum seeking control of continuous stirred tank bioreactors with unknow growth kinetics. Automatica **40**, 881–888 (2004)
15. Mailleret, L., Bernard, O., Steyer, J.P.: Nonlinear adaptive control of bioreactors with unknown kinetics. Automatica **40**, 1379–1385 (2004)
16. Marsili-Libelli, S., Beni, S.: Shock load modelling in the anaerobic digestion process. Ecol. Model. **84**, 215–232 (1996)
17. Marsili-Libelli, S., Muller, A.: Adaptive fuzzy pattern-recognition in the anaerobic-digestion process. Pattern Recognit. Lett. **17**, 651–659 (1996)
18. Mendez-Acosta, H.Q., Campos-Delgado, D.U., Femat, R.: Intelligent control of an anaerobic digester: fuzzy-based gain scheduling for a geometrical approach. In: Proceedings of the 2003 IEEE International Symposium on Intelligent Control, pp. 298–303. Houston, TX (2003)
19. Sachs, J., Meyer, U., Rys, P., Feitkenhauer, H.: New approach to control the methanogenic reactor of a two-phase anaerobic digestion system. Water Res. **33**(9), 973–982 (2003)
20. Speece, R.E.: Anaerobic Biotechnology for Industrial Wastewater. Archae Press, Nashville, TN (1996)
21. Seydel, R.: Practical Bifurcation and Stability Analysis: From equilibrium to Chaos. Springer-Verlag, New York (1994)
22. Shen, S., Veldpuas, F.E.: Analysis and control of a flywheel hybrid vehicular powertrain. IEEE Trans. Control Syst. Tech. **12**(5), 645–660 (2004)
23. Simeonov, I., Stoyanov, S.: Modelling and dynamics compensator control of the anerobic digestion of organic wastes. Chem. Biochem. Eng. **17**(4), 285–292 (2003)
24. Smets, I.Y., Bastin, G.P., Impe, J.F.: Feedback stabilization of fed-batch bioreactors: non-monotonic growth kinetics. Biotech. Prog. **18**, 1116–1125 (2002)
25. Steyer, J.P., Buffiere, P., Rolland, D., Moletta, R.: Advanced control of anaerobic digestion process through disturbances monitor. Water Res. **33**(9), 2059–2068 (1999)
26. Theilliol, D., Ponsart, J.C., Harmand, J., Join, C., Gras, P.G.: On-line estimation of unmeasured inputs for anaerobic wasterwater treatment processes. Control Eng. Pract. **12**, 819–826 (2004)
27. True, H.: On the theory of nonlinear dynamics and its application in vehicle system dynamics. Vehicle Syst. Dyn. **31**, 393–421 (1999)
28. Viel, F., Jadot, F., Bastin, G.: Robust feedback stabilization of chemical reactors. IEEE Trans. Autom. Control **42**(4), 473–481 (1997)
29. Wang, Z.Q., Skogestad, S., Zhao, Y.: Exact linearization control of continuous bioreactors: a comparison of various control structures. In: Proceedings of the 2nd IEEE Conference on Control Applications, pp. 107–112. Vancouver, BC (1993)
30. Wilcox, S.J., Hawkes, D.L. et al.: A neural-network, based on bicarbonate monitoring, to control anaerobic-digestion. Water Res. **29**(6), 1465–1470 (1995)
31. Zhang, Y., Zhu, G.Y., Zamamiri, A.M., Henson, M.A., Hjortso, M.A.: Bifurcation analysis and control of yeast cultures in continuous bioreactos. In: Proceedings of the American Control Conference, pp. 1742–1746. Chicago, IL (2000)